Scaling behavior in submonolayer film growth: A one-dimensional model

J. A. Blackman and P. A. Mulheran
Department of Physics, University of Reading, Whiteknights, P.O. Box 220, Reading RG6 6AF, United Kingdom
(Received 19 April 1996)

The theory of submonolayer thin-film growth has focused on the use of mean-field rate equations as analytic support to Monte Carlo simulations. While these give an excellent account of certain properties, they are totally inadequate for dealing with the distribution of island sizes and the related scaling properties. The reason is the neglect of spatial fluctuations in the mean-field theory. A capture zone construction has recently been introduced by the present authors [Philos. Mag. Lett. **72**, 55 (1995); Phys. Rev. B **53**, 10 261 (1996)] as a way of overcoming this deficiency. The present paper explores and develops this idea in a one-dimensional ''point island'' model. Note that the rate of capture of diffusing monomers is independent of the spatial extent of an island in one dimension. A complete theory for the dynamical and spatial features of the model is developed, including the derivation of a scale-invariant analytic expression for the island size distribution function which agrees very well with the results of Monte Carlo simulations. The implications for two-dimensional systems are discussed. [S0163-1829(96)02839-1]

I. INTRODUCTION

The theory of submonolayer film growth has, until recently, focused on the use of mean-field rate equations as the main analytic partner to Monte Carlo simulations. While this has successfully explained the dynamics of growth, it has become clear that one must look beyond a mean-field treatment to obtain insight into the spatial features of the system and, in particular, to understand the scaling properties that characterize the growth. These properties are manifested most directly in the island size distributions. In this paper, we study an artificial one-dimensional model since this will allow us to demonstrate explicitly the limitations of the mean-field approach *and to go beyond it*. We shall derive a complete analytical theory for the dynamical and spatial features for our model system and, crucially, we shall give a rigorous explanation for the origin of its scaling properties. All of our work is supported by Monte Carlo simulations, and outstanding agreement is found throughout. We begin with a brief survey of the background to this work.

There has been a huge resurgence of interest in the mechanisms of thin film growth over recent years. Electron microscopy has, for a long time, been the main tool for studying surfaces, but the development of scanning tunneling microscopy[1,2] (STM) and surface sensitive electron-diffraction techniques[3–5] such as reflection high-energy electron diffraction now allows one to probe surface details at submonolayer coverages. The theory[6,7] of film growth was developed largely through the sixties and the seventies mainly with reference to three-dimensional island growth, but the refinements in experiments have sparked a renewed interest in the corresponding theory.[8]

Existing growth theories[6,7] define an initial regime in which the density of monomers (isolated atoms on the surface) increases linearly with time until small islands begin to nucleate. As deposition proceeds, the density of islands eventually becomes larger than that of monomers. One enters the so-called aggregation regime which is dominated by the capture of diffusing monomers by existing islands; new nucleation does occur, but much more slowly than in the earlier period. The aggregation regime is finally terminated by the onset of coalescence at 30–40 % coverage.

We start by defining the parameters that characterize the growing islands. One has first of all the number density N_s. This is the number of islands on unit area of substrate that contain s atoms. It will depend on the coverage θ which, for two-dimensional growth, is proportional to the deposition time and the rate of deposition F (assuming evaporation from the surface is negligible). Other quantities of interest are mean island size $\langle s \rangle$, total density of islands N, and the density of monomers N_1. An important parameter in the description is the monomer diffusion rate, D, which depends on both material and temperature.

An important approach to studies of the aggregation regime is the use of dynamical scaling theory. In extensive Monte Carlo simulations, Bartelt and Evans[9–11] showed that the island density takes the form

$$N_s \sim \theta \langle s \rangle^{-2} f(s/\langle s \rangle), \tag{1}$$

where $f(x)$ is a universal scaling function that is independent of coverage and the deposition rate; it does depend on the critical island size, however. This behavior has since been confirmed[12–18] for a number of different models, and has also been observed experimentally in STM studies.[2] The mean quantities $\langle s \rangle$, N, and N_1 display a dependence on coverage and on the ratio $\Re (= D/F)$, which can be described by four exponents:

$$\langle s \rangle \sim \theta^{z} \Re^{\chi}, \tag{2}$$

$$N_1 \sim \theta^{-r} \Re^{-\omega}, \tag{3}$$

$$N \sim \theta^{1-z} \Re^{-\chi}. \tag{4}$$

Values of these exponents have been deduced both from experiment[2,5] and from Monte Carlo simulations,[5,16] and their dependence on critical island size and on the islands' shape (compact or ramified) has been studied.

A popular way to obtain these exponents theoretically is via rate equations.[6,7] These are mean field in nature; that is, they ignore fluctuations in the island distribution on the substrate. Nevertheless, it has been shown that such mean-field predictions are often in very good agreement with computer simulations.[15,16] The usual rate equations describing island growth are

$$\frac{dN_1}{dt} = F - 2K_1N_1^2 - N_1\sum_{s\geqslant 2} K_sN_s, \tag{5}$$

$$\frac{dN_s}{dt} = N_1(K_{s-1}N_{s-1} - K_sN_s), \tag{6}$$

where K_s is the capture kernel for monomers by islands of size s. It is convenient to introduce a diffusion constant D common to all the K_s and to use the amount of material deposited, θ, as the time variable.

$$K_s = D\sigma_s, \quad \theta = Ft. \tag{7}$$

Equations (5) and (6) are specific to growth with a critical island size of 1. Additional terms describing island dissociation can be introduced to accommodate other critical island sizes.

The solution of these equations has been studied via scaling theory[19,20] and by asymptotic methods,[21,22] both in the context of island growth[19,20] and also as applied to other growth problems such as aerosol theory.[22] Generally it is assumed that σ_s has a simple functional dependence on the island size ($\sim s^p$). There has been some controversy over the appropriate value to use for p. The ''point island'' model assumes that p is zero, while an alternative approach adopts the value $\frac{1}{2}$. Paradoxically it appeared that the point island model gave a better prediction of the χ and ω exponents, while the observed dynamic exponents r and z appeared to be consistent with the $p=\frac{1}{2}$ description. The problem was resolved by Ratsch *et al.*[15] referring back to the diffusion based theory of Venables.[23] They proposed that the correct form to take is $\sigma_s \sim (Ns)^{1/2}$. Because N has a logarithmic dependence on θ, there is no change to the prediction of the dynamic exponents by Blackman and Wilding,[19] who solved the general p problem and assigned $p=\frac{1}{2}$ for two-dimensional growth. However, the modification of Ratsch *et al.*[15] does change the exponents χ and ω from their values in the $\sigma_s \sim s^{1/2}$ theory, so that they are now identical to those arising from the point island model. The theory now exhibits internal consistency.

It should be noted that the $\sigma_s \sim (Ns)^{1/2}$ theory represents asymptotic behavior and thus applies only at the higher coverages when the aggregation regime is fully established. When the islands are very small the point island model is an appropriate description. Surveys have been given of the conditions operating at the various stages of coverage by Amar, Family, and Lam[16] and by Evans and Bartelt.[24] It could be argued that using a simple power dependence on s in σ_s is an unnecessary oversimplification. There is the question of whether the aggregation regime lasts long enough for asymptotic behavior to obtain before the coalescence regime takes over. There is also the additional effect at higher coverages of growing islands reducing the area of the substrate available for deposition and, at the same time, themselves receiving direct impact of the new material. However, as long as one is aware of the caveats, it is usually possible, in practice, to observe a tendency toward a particular asymptotic behavior. This is important because obtaining the exponents is a very convenient way of characterizing a particular growth mode. It allows one to identify critical island size, for example,[5] and to distinguish growth dominated by monomer diffusion and capture from other growth processes. The contrast with the exponents obtained in a simple coalescence model[25] has been explored by Blackman[26] using a rate equation formalism.

The rate equation analysis was taken one stage further by Bales and Chrzan.[18] They solved the equations self-consistently so that a form of σ_s was used that was appropriate to all stages of coverage. They also included the effect of direct impact of impinging monomers on existing islands. It was found that the rate equations give a surprisingly accurate prediction of the mean quantities (N, N_1, and $\langle s\rangle$) when compared with computer simulations. However, the description of the island size distribution functions was a complete failure. The reason for this is clear; it is the neglect of spatial fluctuations which are a consequence of the mean-field nature of a rate equation approach.

There have been attempts by Bartelt and Evans[9] and by Amar, Family, and Lam[16] to address the issue of fluctuations through studies of pair-correlation functions and structure factors. An alternative method introduced recently by the present authors[27,28] employs a capture zone approach. The capture zone is the region surrounding an island from which it predominantly acquires the monomers that are responsible for its growth. To a good approximation these capture zones can be identified with Voronoi cells centered on the islands themselves. It was shown[27] that, for heterogeneous growth, the island size distribution function closely mirrors the distribution of Voronoi cell sizes. The scaling of the size distribution occurs because the cell distribution also scales. For homogeneous growth[28] there is the additional complication that new islands are produced during the growth, but it was demonstrated that the Voronoi cell distribution still holds the key to an understanding of the island distribution. The capture zones represent the environment of the growing islands. Monitoring their size distribution provides the information which is absent from mean-field theory. Elements of the capture zone idea are also found in the work of Venables and Ball[29] and of Li, Vidali, and Biham.[4]

Our previous work[27,28] established the importance of capture zones largely from Monte Carlo simulations. In the present work, we shall examine some of these ideas using a one-dimensional analog. It has the advantage that analytic work can be taken much further than in the two-dimensional case, allowing us to probe the process more fully. Furthermore, the logarithmic effects that gave rise to subtleties in two dimensions are absent in this case. One is, of course, concerned that one-dimensional models have their own peculiarities that can obscure issues that are ideally generic. We find that there are no serious pathologies in this case and the model does indeed make transparent issues that are relevant to two dimensions.

The model is studied by Monte Carlo simulations, rate equations, and by the capture zone description. There are three issues: (i) *Growth exponents*. As in two dimensions, we

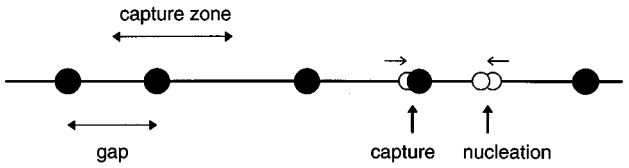

FIG. 1. Summary of the features of the model. Full circles represent static traps; open circles are monomers. A trap is formed (nucleation) when a monomer moves onto a lattice site already occupied by another monomer. A capture zone is the separation of the bisectors of neighboring gaps.

will find excellent agreement between Monte Carlo calculations and the rate equation predictions. (ii) *Mean quantities* ($\langle s\rangle, N, N_1$). Numerical solution of the rate equations gives a fair description of these, but not quite as satisfactory as Bales and Chrzan[18] find in two dimensions. A simple development beyond mean-field theory is necessary to produce excellent agreement with Monte Carlo results. (iii) *Distribution functions*. As we expect, mean-field theory is totally inadequate here. The capture zone description is explored and is shown to account fully for the island size distributions.

The details of the Monte Carlo procedure for one dimension are outlined in Sec. II. In Sec. III we develop the mean-field theory and compare the predictions with the results from the Monte Carlo simulations, first for the exponents and then for $\langle s\rangle$, N, and N_1. The initial signs of the breakdown of mean-field theory appear in the treatment of the average quantities. We show, in Sec. IV, how information about the spatial distribution of islands must be introduced to rectify the deficiencies of mean-field theory. This is developed in detail in Sec. V. In Sec. VI, we address the issue of the island size distribution itself, including a derivation of a scale-invariant analytic expression that relates the island size distribution to the cell distribution. The concluding Sec. VII discusses the implications of this work for the two-dimensional case.

II. MONTE CARLO SIMULATIONS

In the simulations, monomers are deposited at random on a line of L sites, and random diffusive moves of monomers are made one step to the right or the left. $2\Re N_1$ monomer moves are made at random for each time a particle is added. The factor 2 appears because the hopping rate is twice the diffusion rate. When a monomer moves onto a site already occupied by another monomer a trap is formed. Traps remain static; it is only monomers that are mobile. Similarly a monomer that moves onto a site that is occupied by a trap is absorbed. Traps remain one lattice site in extent (a point island model). There is no evaporation of deposited monomers and no dissociation of islands once they have formed (critical island size, $i=1$). The $i=1$ case is the most complex one (because for higher values of i, there is less new nucleation during the aggregation regime), and so the subtle issues are most apparent here. The elements of the model are summarized in Fig. 1.

To focus the study on the deposition/diffusion/capture process alone, the traps were not allowed to grow in size; simply a record was kept of the number of particles absorbed by each trap. This (together with the monomer present at that site at the time of trap nucleation) represents the island size. This allows us to avoid any complication due to direct capture by impact on existing islands which will become significant at higher coverages. In our algorithm, we rejected any direct impacts on the point island traps. An alternative would be to allow immediate capture of any direct impacts. A check was made with the alternative algorithm and it was found that, at coverages involved in the simulations, there was negligible difference in the growth statistics obtained in the two strategies.

In two dimensions, the rate at which diffusing monomers are captured depends on the island size and so the use of a point island model in that case would alter fundamentally the growth process. In one dimension, the capture rate of diffusing monomers is independent of whether one uses a point island model or a model in which the islands are allowed to increase in actual size. In this case, any differences will arise from processes involving direct impact and capture.

Our time scale is coverage defined here as the number of monomers deposited per site. Because the traps do not actually grow, values of θ larger than 1 are possible, while true coverage of the line is only partial. The results of the simulations will be described along with the related theoretical developments.

III. RATE EQUATION ANALYSIS

The starting point for the mean-field analysis is again the rate equations (5) and (6). Using Eq. (7), these can be rewritten as

$$\frac{dN_1}{d\theta} = 1 - 2\Re\sigma_1 N_1^2 - \Re N_1 \sum_{s\geqslant 2} \sigma_s N_s , \tag{8}$$

$$\frac{dN_s}{d\theta} = \Re N_1 (\sigma_{s-1} N_{s-1} - \sigma_s N_s). \tag{9}$$

The total cluster density, which has already been introduced is defined as

$$N = \sum_{s\geqslant 2} N_s . \tag{10}$$

Until now, the rate equations are not dimension specific. Within mean-field theory, the dimension dependence comes in through the quantity σ_s. The peculiarity of one dimension is that σ_s is certainly independent of s at all stages of growth. Now let us consider the deposition of monomers onto a line of length L. To evaluate σ_s, we need to consider the variation of monomer density in the vicinity of a static island. Following Venables[23] and Bales and Chrzan,[18] we define the position dependent monomer density as $n_1(x)$; its average is N_1. We can write down n_1 in terms of a diffusion equation,

$$\frac{\partial n_1}{\partial t} = D\,\frac{\partial^2 n_1}{\partial x^2} + F - D\xi^{-2} n_1 , \tag{11}$$

where ξ is the average distance a monomer travels before being captured by an island or another monomer. So that the equation is consistent with Eq. (5) in the limit $x\to\infty$ when $n_1\to N_1$, we make the identification

$$\xi^{-2}=\left[2\sigma_1 N_1+\sum_{s\geqslant 2}\sigma_s N_s\right]. \tag{12}$$

Combining Eqs. (5) and (10),

$$\frac{\partial(n_1-N_1)}{\partial t}=D\,\frac{\partial^2 n_1}{\partial x^2}-D\xi^{-2}(n_1-N_1). \tag{13}$$

Assuming a quasistatic regime with very small time variations, we obtain for the monomer density as a function of distance x from an island

$$n_1=N_1[1-\exp(-x/\xi)]. \tag{14}$$

The rate of capture of monomers is $2D[dn_1/dx]_{x=0}$, where the factor of 2 is included because they arrive from both sides of the trap. This is to be compared with the capture rate defined as $D\sigma_s N_1$, giving $\sigma_s=2/\xi$ independent of s as expected. The above argument applies for $s\geqslant 2$; for monomer monomer capture, the argument has to be modified slightly, but the behavior $\sigma_1=2/\xi$ still applies. At this stage it is convenient to anticipate that modifications to mean-field theory will be necessary and to introduce correction factors α and β into the capture kernels, and write $\sigma_1=2\alpha/\xi$ and $\sigma_s=\sigma$ (for $s\geqslant 2$) with $\sigma=2\beta/\xi$. Using these definitions and Eq. (12), one obtains

$$\sigma_1=4\alpha(2\alpha N_1+\beta N), \tag{15a}$$

$$\sigma=4\beta(2\alpha N_1+\beta N), \tag{15b}$$

$$\xi^{-1}=2(2\alpha N_1+\beta N). \tag{15c}$$

Assuming that we are in the regime where $N\gg N_1$ and that α and β have the mean-field values of unity, then σ_1 and σ are proportional to N, while the mean-free path, ξ, is just half the trap separation. The techniques of scaling theory can then be applied to obtain growth exponents. Following the standard methods,[15,16,19] the following values for the exponents are obtained:

$$\omega=1/2,\quad r=1/2,\quad \chi=1/4,\quad z=3/4. \tag{16}$$

We have defined $\langle s\rangle$ as

$$\langle s\rangle=N^{-1}\sum_{s\geqslant 2} sN_s=(\theta-N_1)/N. \tag{17}$$

An alternative commonly used definition of the mean size which involves the second moment of the distribution function will give identical growth exponents.

The Monte Carlo simulations are used first to test the growth exponent behavior predicted by Eqs. (2)–(4), (16). The deposition was done on a line of $L=2\times10^5$ sites and for three values of $\mathfrak{R}$: 0.5×10^5, 0.5×10^6, and 0.5×10^7. The results were average over 10 runs in each case. The trap density N, monomer density N_1, and average trap size $\langle s\rangle$ are plotted as a function of $\theta\,(=Ft)$ in Figs. 2–4, respectively. For convenience, the quantities scaled according to the mean-field predictions are also plotted. The scaled plots are seen to be in accord with the predictions; in each of the figures they asymptote to a limit that is independent of θ and $\mathfrak{R}$. The range of θ is more restricted at the higher values of $\mathfrak{R}$, because all monomers are eventually taken out of the system by the traps at a faster rate than new ones are deposited. A larger L is necessary to extend the range. At the largest values of θ reached in the simulations, the real coverages (as opposed to θ) are about 14%, 6%, and 2% for the three deposition rates.

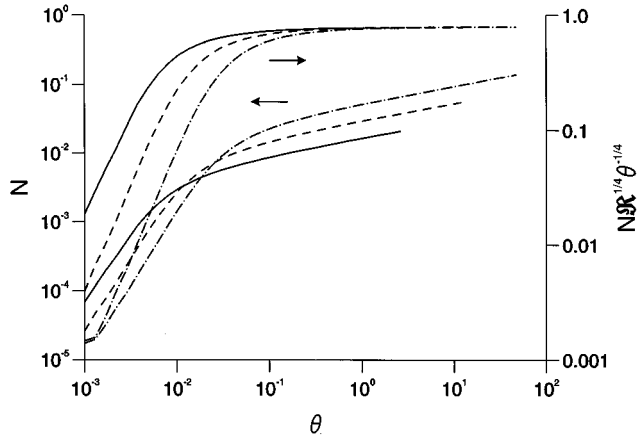

FIG. 2. Trap density N as a function of $\theta\,(=Ft)$ for three values of $\mathfrak{R}(0.5\times10^5$ chain line; 0.5×10^6 broken line; 0.5×10^7 full line). Second group of plots shows the scaled trap density.

Now let us examine the capture kernels σ_1 and σ that have been employed in the rate equation formalism. At the moment they contain two free parameters α and β each of which is expected to be unity if mean-field theory applies. From the data displayed in Figs. 2 and 3, we can calculate $dN_1/d\theta$ and $dN/d\theta$. Then all quantities in the rate equations (8) and (9) are known except for α and β themselves. Thus, a comparison of the rate equations with the simulation data enables us to extract α and β and any θ dependence they might show. The results of the calculation are shown in Fig. 5. At early time both are considerably above unity; this is not remarkable because the assumptions (e.g., quasistatic regime) implicit in the derivation of the expressions for the capture kernels do not apply at this stage. At larger θ, when aggregation conditions are believed to operate, interesting behavior is observed. α, the coefficient in σ_1, does settle

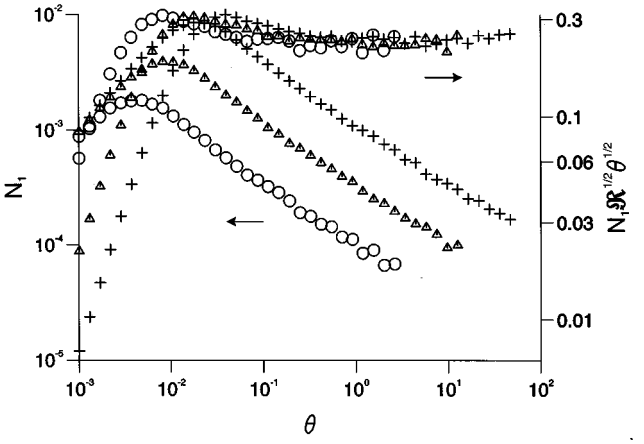

FIG. 3. Monomer density N_1 as a function of $\theta\,(=Ft)$ for three values of $\mathfrak{R}(0.5\times10^5$ crosses; 0.5×10^6 triangles; 0.5×10^7 circles). Second group of plots shows the scaled monomer density.

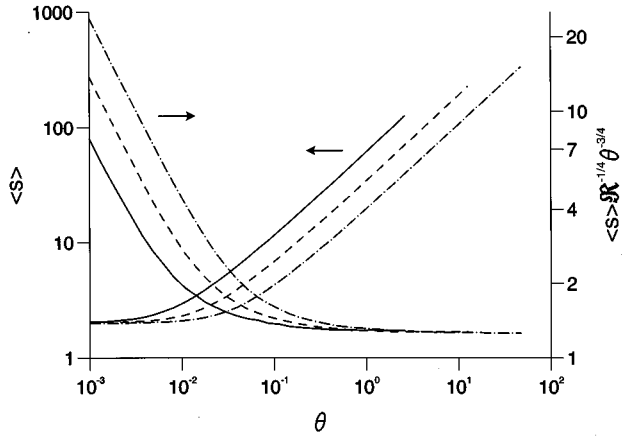

FIG. 4. Mean trap size $\langle s \rangle$ as a function of $\theta\,(=Ft)$ for three values of $\Re$ (0.5×10^5 chain line; 0.5×10^6 broken line; 0.5×10^7 full line). Second group of plots shows the scaled trap size.

down to approximately one, while β, the coefficient in σ, quite definitely approaches a value that is larger than unity. There is some evidence that α may be marginally less than one but, because of noise in the data, it is not a point that is worth pursuing. Even with the noise in the data, it is quite clear that β lies in the range 1.3–1.4. From evidence to be presented later, we will take the best of β as 1.389. Although this is our first evidence of departures from mean-field behavior, it has not influenced the predictions of the exponents because all that was required in their derivation was sustained constant values for α and β; their absolute values were not important.

To present these observations in another way, the rate equations are now solved numerically using values of α and β of 1 and 1.389, respectively. The results for N and $\langle s \rangle$ are shown in Fig. 6 along with the data points from the Monte Carlo simulations and a numerical solution of the rate equations with both coefficients set to unity. Monte Carlo data for N_1 is more noisy because of the small number monomers remaining at the later stages of the aggregation regime, and does not yield conclusive results in the present comparison. The comparison displayed in the plots for N and $\langle s \rangle$ is quite conclusive, however. Clearly the mean-field predictions of

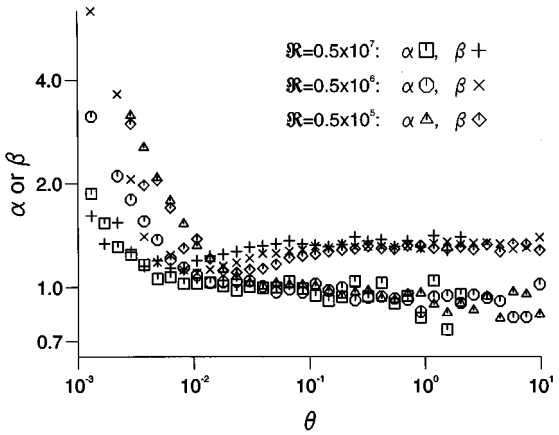

FIG. 5. Coefficients α and β versus $\theta\,(=Ft)$. Data is shown for three values of $\Re$.

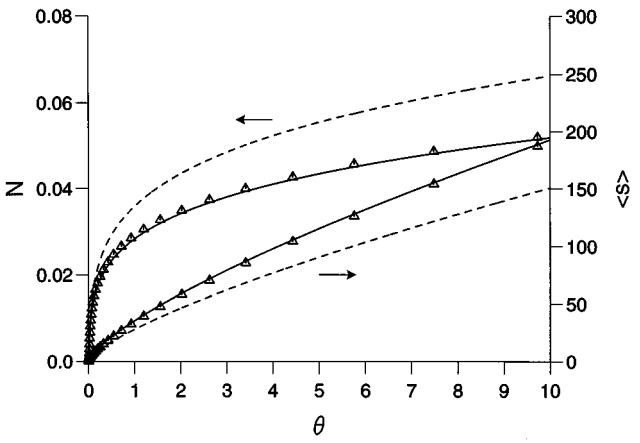

FIG. 6. Trap density N and mean trap size $\langle s \rangle$ as a function of $\theta\,(=Ft)$. Data points are from Monte Carlo simulations. Lines are from numerical solution of the rate equations with $\alpha=1.0$ and β equal to 1.0 (broken lines) and 1.389 (full lines).

the capture kernels is not correct. Once the amendment is made of using the value of β that is different from unity, the agreement is excellent. The use of the rate equations themselves is successful even though they are mean field in nature; it is necessary though to use a value of σ which can only be derived, as we shall show later, by going beyond mean-field theory. In two dimensions, by comparison, Bales and Chrzan[18] show that corrections to mean-field theory are negligible at this stage.

We finish this section by examining the distribution function N_s. The time evolution found from Monte Carlo simulations is shown by the solid curves in Fig. 7. The results from the numerical solution of the rate equations are shown in the same figure. One set of plots displays the results when β is taken as unity and the other is the data obtained when $\beta=1.389$. Clearly the modified value of β does bring some improvement but, as in two dimensions, the rate equation predicts distribution functions that are much too narrow.

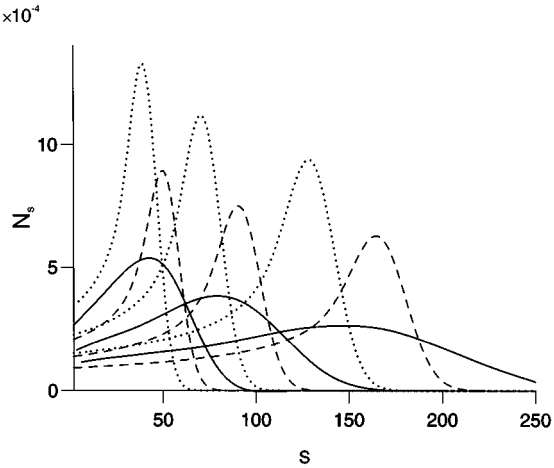

FIG. 7. Distribution function N_s versus s for three coverages (θ=1.19, 2.62, 5.76—plots left to right). Full lines: Monte Carlo simulations; other plots are results from numerical solution of the rate equations with $\alpha=1.0$ and β equal to 1.0 (dotted lines) and 1.389 (broken lines).

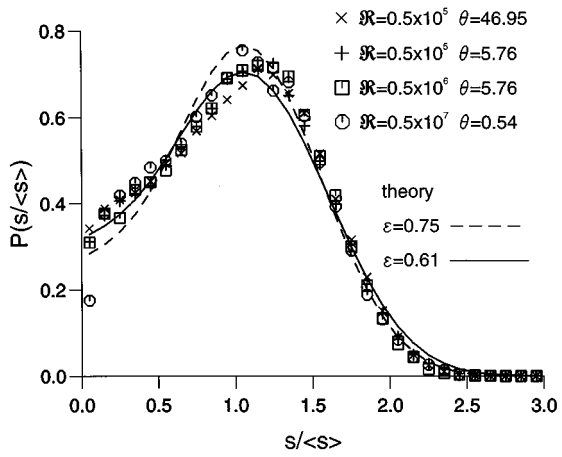

FIG. 8. Scaled distribution $P(S)$ from Monte Carlo simulations plotted for several values of θ and $\Re$. Full and broken lines are theoretical distribution functions from Eq. (38): as discussed in Sec. VI.

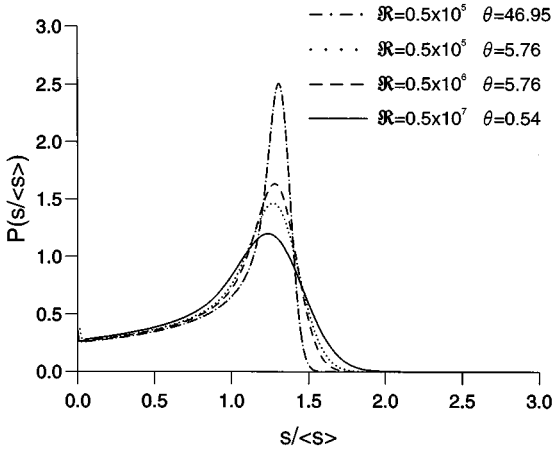

FIG. 9. Scaled distribution $P(S)$ from numerical solution of rate equations ($\alpha=1.0$ and $\beta=1.389$) for same values of θ and $\Re$ used in Fig. 8.

The scaling properties of the distribution functions have been well studied in two dimensions and, not surprisingly, scaling behavior is exhibited in the one-dimensional model. This is illustrated in Fig. 8 where the scaling properties of the Monte Carlo results are shown. An equivalent way to study the scaling behavior expressed in Eq. (1) is to write N_s as a function of the scaled variable S, where $S=s/\langle s\rangle$, and to normalize it so that it is a probability function; we denote the function by $P(S)$:

$$\int P(S)dS=\int SP(S)dS=1. \tag{18}$$

Note that P describes the distribution of traps only (monomers are excluded; i.e., there is no $s=1$). In Fig. 8, $P(S)$ shows the characteristic scaling behavior for a range of values of θ and $\Re$.

Although we have already demonstrated that the rate equations do not give a correct description of the distribution function, it is instructive to show the $P(S)$ obtained from their numerical solution. The $\beta=1.389$ results are displayed in Fig. 9. The rate equations do not give scaling behavior. It is true that scaling theory arguments can be used to derive the growth exponents, but the assumption is made that one is in a regime where $N_1\sim t^{-r}$, and that is only valid in the asymptotic limit. Thus, scaling to a common function does occur but only at small $s/\langle s\rangle$, where $\langle s\rangle\sim t^z$.

IV. BEYOND MEAN-FIELD THEORY

The rate equations ignore spatial fluctuations in N and N_1 and, in that sense, they are a type of mean-field theory. We can begin to introduce the effect of fluctuations if we recognize that the actual monomer density n_1 is a strong function of position on the line and is highly sensitive to the local trap separation.

In the aggregation regime, when the monomer density is in an approximately steady state, $n_1(x)$ between a pair of islands situated at $x=0$ and $x=y$ is obtained from the diffusion equation,

$$D\frac{d^2n_1}{dx^2}+F\approx 0. \tag{19}$$

That is,

$$n_1(x)=\tfrac{1}{2}\Re^{-1}x(y-x), \tag{20}$$

and the total number of monomers in the gap is given by $\overline{n_1}=y^3/12\Re$. If $\overline{n_1}$ is averaged over all gaps along the line, we can obtain the mean monomer density (N_1 in the notation already introduced): $N_1=\langle y^3\rangle N/12\Re$. The mean gap size is given by $\langle y\rangle=N^{-1}$. Introducing scaled variables, $Y=y/\langle y\rangle$, we obtain the relation

$$12N^2N_1\Re=\langle Y^3\rangle. \tag{21}$$

To check the validity of this relation, the left- and right-hand sides of Eq. (21) are plotted against θ in Fig. 10 using data from the Monte Carlo simulations at three values of $\Re$. The approach to the common limit in the aggregation regime is seen quite clearly. Also the fact that the common limit is the same for each $\Re$ implies that the distribution of gap sizes is a function that exhibits scaling properties.

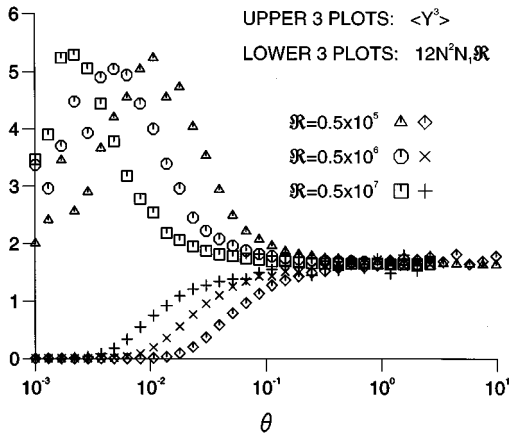

FIG. 10. Plots of $\langle Y^3\rangle$ and $12N^2N_1\,\Re$ against $\theta\,(=Ft)$, for three values of $\Re$.

The quantity $\langle Y^3 \rangle$ contains details about the spatial distribution of traps that is absent from mean-field theory. This extra information will provide us with an estimate of the coefficient β which has been observed to take a value different from the mean-field prediction of unity. The rate of capture of monomers by a trap at $x=0$ is given by $2D[dn_1/dx]_{x=0}=D\Re^{-1}\langle y\rangle$. As before the factor 2 arises because of capture from left and right. We have averaged over all gap sizes. Identifying the capture rate with $D\sigma N_1$, noting that $N=\langle y\rangle^{-1}$, and using Eq. (21), we obtain an expression for σ,

$$\sigma = 12N/\langle Y^3 \rangle. \tag{22}$$

A comparison with Eq. (15b) in the aggregation regime where $N \gg N_1$ leads to the identification

$$\beta = [3/\langle Y^3 \rangle]^{1/2}. \tag{23}$$

The common value of $\langle Y^3 \rangle$ in Fig. 10 is about 1.6 (a more accurate estimate will be given in the next section), which is consistent with the value of β used earlier. From Eq. (15c), it can be seen that the physical effect of a β larger than 1 is to reduce the mean diffusion path to less than its mean-field value. Since $\langle Y^3 \rangle$ is proposed as a universal number, one would like to be able to obtain it from theory rather than from a Monte Carlo simulation. This entails an investigation of the distribution function for the gaps between the traps.

V. THE GAP DISTRIBUTION FUNCTION

Consider a line of length L with trap density N. There are a total of M $(=NL)$ traps on the line. It is convenient to define two probability distributions for the gaps between traps. $F_M(y)$ is the number of gaps in the range y to $y+dy$. The moments of $F_M(y)$ are

$$\mu_M(p) = \int_0^\infty y^p F_M(y)\, dy \tag{24}$$

and obviously $\mu_M(0)=M$ and $\mu_M(1)=L$.

A scaled distribution function $G(Y)$ is also introduced where $Y=y/\langle y\rangle$. This is the probability distribution for gap widths normalized so that

$$\int_0^\infty G(Y)\, dY = \int_0^\infty Y G(Y)\, dY = 1. \tag{25}$$

The moments of $G(Y)$ are defined

$$Q_p = \int_0^\infty Y^p G(Y)\, dY. \tag{26}$$

Q_0 and Q_1 are both 1 and it is Q_3 that is relevant to the discussion in the previous section.

The relationship between the two distribution functions is summarized by the expressions

$$F_M(y) = MNG(Y), \tag{27}$$

$$\mu_M(p) = MN^{-p}Q_p, \tag{28}$$

and $Y=y/\langle y\rangle = Ny$

We proceed by considering $F_M(y)$ and the effect on it of a single new nucleation. The probability of a new nucleation at position x is proportional to $n_1(x)^2$ and the probability of new nucleation somewhere within a gap of width y will be proportional to $\int_0^y n_1(x)^2 dx$; that is, to y^5. The monomer density is given in Eq. (20). Normalizing these values, the probability that the new nucleation will take place somewhere in a particular gap of width y is $y^5/\mu_M(5)$. The probability, given a particular gap, that it will take place between x and $x+dx$ within that gap is $\psi(x/y)dx/y$, where

$$\psi(\lambda) = 30\lambda^2(1-\lambda)^2. \tag{29}$$

The effect of a new nucleation can be described by the equation

$$F_{M+1}(y) = F_M(y)[1-y^5/\mu_M(5)] + \int_y^\infty F_M(z)[z^5/\mu_M(5)] \times [\psi(y/z)+\psi(1-y/z)]\, dz/z. \tag{30}$$

The first term on the right-hand side gives the number of gaps of size y remaining after the new nucleation. The second term gives the number of new gaps of size y being created from larger gaps of size z. There are two parts to the second term because a size y gap is created by new nucleation both at y and at $z-y$.

Using the relation, $F_{M+1}(y)-F_M(y) = N[2G + Y\, dG/dY + O(1/M)]$, together with the symmetry $\psi(\lambda)=\psi(1-\lambda)$, an equation for the scaled probability can be derived from Eq. (30),

$$Y\, dG/dY + (2+Y^5/Q_5)G = 2\int_Y^\infty [Z^5 G(Z)/Q_5]\psi(Y/Z)Z^{-1}\, dZ. \tag{31}$$

A useful relation between moments can be obtained straightforwardly from Eq. (31),

$$(p-1)Q_pQ_5 = (1-2A_p)Q_{p+5}, \tag{32}$$

where

$$A_p = \int_0^1 \lambda^p \psi(\lambda)\, d\lambda. \tag{33}$$

With the specific form of ψ from Eq. (29), the following relation emerges:

$$Q_pQ_5 = \left(\frac{15}{p+3} - \frac{24}{p+4} + \frac{10}{p+5}\right) Q_{p+5}. \tag{34}$$

A consideration of the $Y\to\infty$ limit of Eq. (31) shows that the distribution function has the form $G(Y) = H(Y)\exp(-Y^5/5Q_5)$. Note that this general behavior is independent of the precise polynomial expression for the function ψ. The form of the exponential tail arises because the probability of new nucleation within a gap is proportional to the size of that gap to the fifth power. The details of the nucleation probability within a gap determine the function H. We are unable to obtain an analytic solution for $G(Y)$ in our model, but we can make the following additional statements about the form of $H(Y)$ by examining Eq. (31) in various limits. In particular, $H(Y) = 15(Q_2/Q_5)Y^2$ in the small Y limit and, as $Y\to\infty$, $H(y)\sim Y^{-2}$.

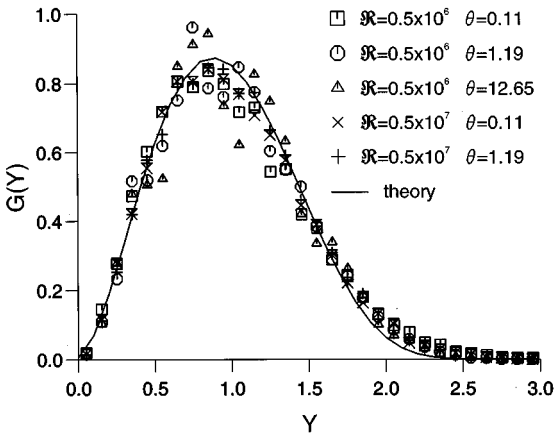

FIG. 11. $G(Y)$ as a function of Y for several values of $\Re$ and θ from the Monte Carlo simulations (data points). The theoretical curve is shown by the full line.

As an exactly soluble model, although an artificial one, it is interesting to study $G(Y)$ when $\psi(\lambda)=1$. In this case, the weighting according to gap size is included, but nucleation within the gap can occur anywhere with equal probability. Details are given in the Appendix.

The gap distributions are recorded over a range of values of θ during the Monte Carlo simulations. These are shown by the data points in Fig. 11. Scaling behavior is evident. We wish to compare these plots with the theoretical distribution given implicitly by Eq. (31). Rather than solve the integrodifferential equation numerically, we prefer to obtain $G(Y)$ by a statistical method. A line of length L is taken and an array of point on the line is generated. Each new point is introduced via weighted random number generation. First, a pair of existing points is selected between which to introduce the new one. The selection is weighted by the fifth power of the separation of the points. Then the actual position in the gap for insertion is selected with weighting given by the function ψ in Eq. (29). This was done for a final set of point densities along the line ranging from 1–10 %, and for line lengths between 1000 and 10 000. Each configuration was averaged over 10 000 runs. The results for $G(Y)$ obtained for the different configurations were indistinguishable, and are shown by the continuous line in Fig. 11. As a check that $G(Y)$ thus obtained agrees with the analytic result of Eq. (31), we evaluated the moments and compared them for consistency with the prediction of Eq. (34). The moments from the zeroth to the eighth are reproduced in Table I. The second column shows Q_p obtained numerically from the theoretical curve in Fig. 11. For the third column, Eq. (34) has been used to calculate higher moments from the lower ones. One can see the good agreement.

In comparing the Monte Carlo data with the theoretical curve, one can see some slight broadening in the former; The Monte Carlo data tends to lie a little above the tail and slightly below the peak of the theoretical curve. It would be surprising if there was a perfect fit, because we have been proceeding on the assumption that the monomer density is in a steady state. Obviously the very close agreement in Fig. 11 between the data points and the theory curve indicates that this is a very good approximation and the broadening effects can probably be ascribed to the very slow variation in monomer density.

TABLE I. Zeroth through eight moments.

p	Q_p	Q_p [from Eq. (32)]
0	1.0	
1	1.0	
2	1.178±0.002	
3	1.555±0.003	
4	2.237±0.005	
5	3.44±0.01	
6	5.59±0.03	5.58±0.02
7	9.52±0.06	9.46±0.05
8	16.83±0.15	16.64±0.09

From the table, our best theoretical estimate of Q_3 is 1.555. This is just the $\langle Y^3\rangle$ that appeared in Eq. (23) and provides the value of β of 1.389 that we used in the discussions of the rate equation and the plots in Fig. 6.

In this section we have defined an abstract problem about the distribution of points along a line according to a particular algorithm. A distribution function has been obtained and it has been shown that this function agrees in essentials with the distribution of gaps observed in the one-dimensional deposition model. In the following section, it will be shown that this development provides a basis for overcoming the shortcomings of mean-field theory.

VI. CAPTURE ZONE AND TRAP DISTRIBUTIONS

Our previous work in two dimensions[27,28] demonstrated the key role played by capture zones in determining the distribution of island sizes. The capture zones were identified by a Voronoi cell construction.[30] The equivalent construction for obtaining the capture zone of a particular trap in one dimension is the trivial bisection of the gaps to its left and right. If there is no correlation between the sizes of the two gaps, then we would expect that a simple convolution of the gap distribution function would yield the capture zone distribution, $V(Y)$,

$$V(Y)=2\int_0^{2Y} G(Z)G(2Y-Z)dZ. \tag{35}$$

We can use scaled variables immediately because the mean gap and capture zone sizes are identical. The prefactor 2 ensures a normalization for $V(Y)$ similar to that for $G(Y)$ in Eq. (25). One might argue that the nucleation process tends to produce correlations; new nucleation is weighted toward the center of existing gaps and, therefore, one might expect that the gaps to the left and right of a new island are of similar size. However, any such correlations that are present with an existing island will tend to be destroyed when a new nucleation occurs in its vicinity. It is likely that the second effect will dominate and Eq. (35) will be valid to a very good approximation.

This conjecture is tested by evaluating $V(Y)$ numerically using Eq. (35) and the theoretical $G(Y)$ of Fig. 10. The results are compared with data on the capture zones from the

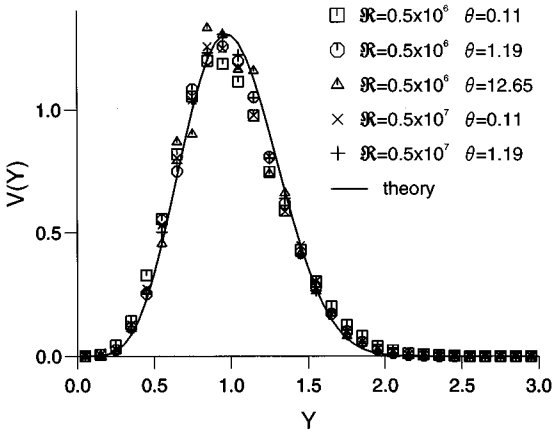

FIG. 12. $V(Y)$ as a function of Y for several values of $\Re$ and θ from the Monte Carlo simulations (data points). The theoretical curve [from Eq. (35)] is shown by the full line.

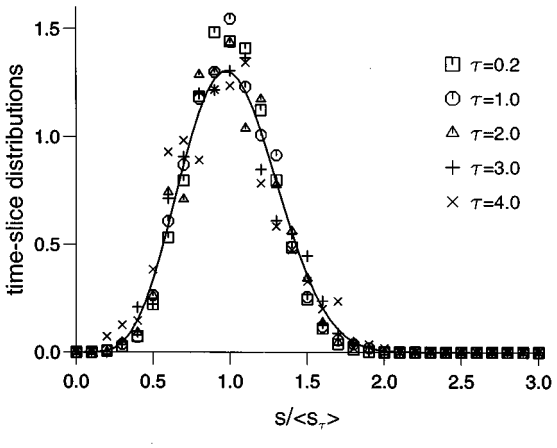

FIG. 13. Distribution functions at time t for islands that were nucleated in time slice of width $\Delta\tau=0.1$ at time τ (data points). Full line is $V(Y)$ from Fig. 12.

Monte Carlo simulations for several values of θ and $\Re$ in Fig. 12. The excellent agreement demonstrates the validity of ignoring correlations and, through Eq. (35), gives us a direct means of evaluating the capture zone distribution.

In the present simplified model, the traps remain static at essentially zero size. The capture zone construction is done by a trivial bisection of the gaps between the traps. In a model where trap growth is included, the capture zones are constructed by the simple extension of bisecting the gaps between the island edges.

Now let us construct a heuristic argument to relate the capture zone distribution, $V(Y)$, to the island size distribution, $P(S)$. This is based on the observation[27,28] in two dimensions that the rate of growth of an island is proportional to its capture zone. We wish to describe the island size distribution at time t, and consider first those islands that were nucleated in a time interval $d\tau$ at time τ $(0<\tau<t)$. Since mean-field behavior has been shown to give a good account of the time dependence of the island density, N, we can use Eqs. (4) and (16) to deduce that the number of new islands created in this time interval is given by $dN\sim\tau^{-3/4}d\tau$.

We follow the evolution of the islands formed in the time slice at τ and denote their average size at subsequent times by $\langle s_\tau\rangle$. Now, given our earlier observations, we assume that rate of change of this quantity at any time t' $(\tau<t'<t)$ is proportional to the mean capture zone size $\langle y\rangle$, and $\langle y\rangle$ itself is proportional to N^{-1}. With the N dependence on time noted above, $d\langle s_\tau\rangle/dt'\sim t'^{-1/4}$, leading to the relation, $\langle s_\tau\rangle=kt^{1/4}[1-(\tau/t)^{3/4}]$, as an estimate of the mean size at time t of islands nucleated at τ; k is a constant. We prefer to write the relation as

$$\langle s_\tau\rangle=kt^{3/4}[1-(\tau/t)^{\varepsilon}], \tag{36}$$

with, for the moment, $\varepsilon=3/4$.

Now let us make the rather drastic assumption (to be justified later) that the size distribution of islands created in a particular time slice maintains throughout the subsequent evolution a functional form similar to that of the capture zone distribution; that is, it is proportional to $V(s/\langle s_\tau\rangle)$. We can then add the contribution from each time slice (dN islands originate in an interval $d\tau$) to get the complete island size distribution.

$$P'(s,t)=A\int_0^t d\tau\, V(s/\langle s_\tau\rangle)[\tau^{-3/4}/\langle s_\tau\rangle]. \tag{37}$$

At the moment, we are using the unscaled distribution denoted by P'. The relation between the scaled and unscaled functions is $P(s/\langle s\rangle)ds/\langle s\rangle=P'(s,t)ds$. In Eq. (37), A is a normalization constant.

The constants, A and k, can be determined by satisfying the normalization conditions, Eq. (18), which yield $4At^{1/4}=1$ and $3/4kt^{3/4}=\langle s\rangle$, where $\langle s\rangle$ is the mean size of the complete set of islands. The final result after these substitutions is

$$P(S)=\frac{1}{(1+4\varepsilon)}\int_0^1 V\left[\frac{4\varepsilon S}{(1+4\varepsilon)(1-\lambda)}\right]\frac{d\lambda}{(1-\lambda)\lambda^{[1-1/(4\varepsilon)]}}. \tag{38}$$

Using $\varepsilon=\frac{3}{4}$, the capture zone distribution function $V(Y)$ from Eq. (35) and Fig. 12 and numerically integrating Eq. (38), we obtain the plot shown by the broken line in Fig. 8. Given the rather drastic (and, as yet, to be substantiated) assumptions used in deriving Eq. (38), the agreement between this plot and the Monte Carlo data is remarkably good. There is a possible concern that the discussion given is invalid at early times before the aggregation regime is established. From Figs. 2–4, it can be seen that the aggregation regime is established very early ($\theta\sim10^{-2}$) and so any doubt of this nature exists only for λ in Eq. (38) close to zero. Because $[1-1/(4\varepsilon)]<1$, only a very small contribution to the integral comes from this region and so preaggregation regime influences are negligible.

Let us now examine rather more closely the validity of the two main assumptions made in deriving Eq. (38). A key ingredient was the supposition that the size distribution at time t of islands originating within a time slice at τ was given by $V(s/\langle s_\tau\rangle)$, where $\langle s_\tau\rangle$ is the average size at t of islands from that time slice. We monitored the evolution of islands from a range of time slices and display some sample distribution functions in Fig. 13. The line curve is $V(Y)$ for

comparison. The Monte Carlo data sets used in the test correspond to $t=5.0$ (in units of θ) and $\Re=0.5\times10^6$. The data for each value of τ is gathered from a time slice of width $\Delta\tau=0.1$ (in the units of θ). It can be seen that the assumption made is a remarkably (and perhaps surprisingly) good one. If anything the time slice distributions are marginally narrower than $V(Y)$ at the earlier values of τ, but any discrepancy between the Monte Carlo data and the theoretical function is small.

Now let us examine, the validity of Eq. (36) with $\varepsilon=0.75$. The mean values $\langle s_\tau\rangle$ from each time slice are shown as a function of τ by the box symbols in Fig. 14. Again, the time observations are made is $t=5.0$. The full curve indicates the fraction of the total number of islands present at t that have been nucleated at time τ. The ratio $\langle s_\tau\rangle/[1-(\tau/t)^{0.75}]$ is shown by the circles and is seen to be fairly constant, although there is a systematic fall off in the curve up to $\tau\sim2.0$ during which time $\sim80\%$ of the islands have formed.

We can argue that Eq. (36) with $\varepsilon=3/4$ overestimates the mean size of the environment of an island immediately after it is formed. When an island forms in a gap between existing islands, its capture zone size is half of the size of the gap. At the simplest level, one would argue that the average capture zone size of a newly formed island is half the average capture zone size of existing islands, and as the newly formed island evolves it also eventually sees the average environment. One must remember, however, that new islands are more likely to form in the larger gaps; to be precise the probability of the formation taking place in a gap of size y is proportional to y^5. This would lead us to predict that the mean gap size that a newly formed island finds itself in is equal to Q_6/Q_5, where these moments are defined in Eq. (26). The average capture zone size of a newly formed island will be half of this.

We will now try to incorporate this extra information into the free parameter ε that we have left ourself in Eq. (36). Remember that equation has been obtained from the assumption that $d\langle s_\tau\rangle/dt$ is proportional to the average capture zone size. For $t\gg\tau$ and arbitrary $\varepsilon>0$, $d\langle s_\tau\rangle/dt=3/4kt^{-1/4}$; this implies that the islands are growing in an average environment whose size $\sim t^{-1/4}$; this time dependence was one of the valid predictions of mean-field theory. At time τ, when the islands are just formed, Eq. (36) yields $d\langle s_\tau\rangle/dt=3/4k\tau^{-1/4}(4\varepsilon/3)$. The factor $4\varepsilon/3$ is a convenient way of representing the reduction in size of the environment of the newly formed islands compared with the average environment that exists at that time. We identify that factor with $Q_6/(2Q_5)$, and deduce that

$$\varepsilon=\frac{3Q_6}{8Q_5}. \tag{39}$$

Referring to Table I, this leads to a value of ε of 0.61.

The triangular data points in Fig. 14 display the ratio $\langle s_\tau\rangle/[1-(\tau/t)^{0.61}]$. The closeness to constancy of the plot is evidence that the argument is basically a correct one. Finally, we repeat the calculation of Eq. (38) with the new value of ε and display the results by the continuous curve in Fig. 8. There is a distinct improvement on the previous calculation over most of the plot apart from some minor deviation in the tail above $s/\langle s\rangle\sim1.8$.

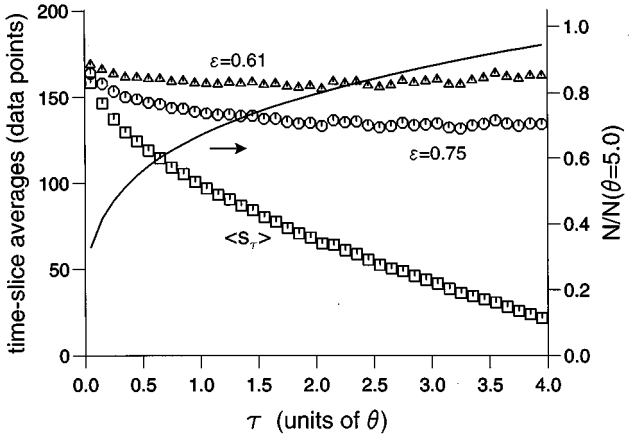

FIG. 14. Mean size of islands $\langle s_\tau\rangle$, at time t that were nucleated in a time slice of width $\Delta\tau=0.1$ at time τ (box symbols). $\langle s_\tau\rangle/[1-(\tau/t)^\varepsilon]$ is shown for $\varepsilon=0.75$ (circles) and $\varepsilon=0.61$ (triangles). Full curve indicates fraction of total number of islands at t (in units of θ) that have been created by time τ.

We have thus fully overcome the shortcomings of mean-field theory. An analytic expression has been obtained for the island size distribution function that is in excellent agreement with the Monte Carlo simulations. The expression, Eq (38), relates the trap sizes to their spatial distribution and provides a first-principles derivation of the scaling properties.

VII. CONCLUSIONS

The key injection into the theory is the one-dimensional equivalent of Voronoi cells. There are two comments stemming from this, one qualitative, the other quantitative. The qualitative statement that an island traps on average those monomers within its capture zone is, of course, an exact one purely on symmetry grounds. In two dimensions, the polygonal construction of the capture zones is not exact in the same sense but is likely to be (and has been demonstrated to be[27,28]) true to a very good approximation. It is also to be expected that the rate of growth of an island will be proportional to its capture zone. However, in a homogeneous model like the current one where an island is evolving through an ever changing environment due to new deposition, one might anticipate that there would be some broadening out of the distribution due to the random nature of the process. Instead a distribution that mirrors that of the capture zones is maintained in a very robust fashion as was seen in Fig. 13.

Similar observations have already been made in the two-dimensional case.[27,28] A main objective of the current work has been to address these issues in a more quantitative way using simple diffusion theory coupled with an analytic treatment of the spatial distribution of points along a line. The essential point in the development is the quasistatic approximation; the time variation of the monomer density, N_1, is slow compared with the rate of introduction of new monomers into the system. The approximation is, of course, a good one and it has enabled us to obtain an overall picture of all aspects of the growth process including the island size distribution function itself. Any departures from the approxi-

mations assumed are small ones and will produce only very minor changes in the finer details.

The scaling that is ubiquitous in the growth phenomena has been tied to the scaling that occurs in the capture zone distribution function. This has enabled us to derive an analytic form for the island size distribution function, Eq. (38), that exhibits scaling without it having to be implanted because of empirical observation.

What are the implications for two dimensions? In principle, the ideas that are underlying the current development are transferable. We know that the mean-field theory for the exponents operates in that case. The need to introduce the correction factor, β, into the discussion of the monomer mean free path, ξ, is perhaps a detail special to one dimension. This necessity is probably connected with the fact that a monomer, once deposited, is strictly confined to move in the gap between two traps. There is no analogous constriction in two dimensions, and this could be the reason why Bales and Chrzan[18] had no need to introduce such a correction.

The capture zone and island size distributions have already been related for heterogeneous[27] and for homogeneous[28] growth in two dimensions by means of Monte Carlo simulations and canonical expressions for the Voronoi cell behavior.[31,32] In this case, of course, there is a size dependence to the σ_s that appears in the rate equations as opposed to the point island behavior of one dimension. That is a mean-field theory complication however and, in the capture zone model, both types of behavior are incorporated in the statement that the rate of growth of an island is proportional to its cell area. The outstanding issues are precise forms for the capture zone and island size distribution functions which contain scaling from first-principles arguments. Both of these issues have been answered in the one-dimensional model and work is currently underway to adapt this approach to the two-dimensional case.

ACKNOWLEDGMENTS

This work was supported in part by the SERC (now EPSRC) through Grant no. GR/H65221-C32. The authors would like to acknowledge interesting discussions with Charles Clement about analogous problems in aerosol theory.

APPENDIX

If $\psi(\lambda)=1$ so that the probability of nucleation is uniform within a gap, then Eq. (31) can be recast into a differential equation

$$Y\ d^2G/dY^2+(3+Y^5/Q_5)dG/dY+7Y^4G/Q_5=0. \tag{A1}$$

The solution of this, normalized to 1 for the zeroth moment is

$$G(Y)=K\ \exp(-Y^5/5Q_5), \tag{A2}$$

where the constant and the various moments can be written in terms of γ functions.

$$K=\frac{5\Gamma\left(\frac{2}{5}\right)}{\Gamma\left(\frac{1}{5}\right)^2}, \tag{A3}$$

$$5Q_5=\left[\frac{\Gamma\left(\frac{1}{5}\right)}{\Gamma\left(\frac{2}{5}\right)}\right]^5, \tag{A4}$$

and generally

$$Q_p=\left[\frac{\Gamma\left(\frac{1}{5}\right)}{\Gamma\left(\frac{2}{5}\right)}\right]^p\frac{\Gamma\left(\frac{p+1}{5}\right)}{\Gamma\left(\frac{1}{5}\right)}. \tag{A5}$$

[1] Y. W. Mo, J. Kleiner, M. B. Webb, and M. Langally, Phys. Rev. Lett. **66**, 1988 (1991).
[2] J. A. Stroscio and D. T. Pierce, Phys. Rev. B **49**, 8522 (1994).
[3] H.-J. Ernst, F. Fabre, and J. Lapujoulade, Phys. Rev. B **46**, 1929 (1992).
[4] W. Li, G. Vidali, and O. Biham, Phys. Rev. B **48**, 8336 (1993).
[5] J.-K. Zuo, J. F. Wendelken, H. Dürr, and C.-L. Liu, Phys. Rev. Lett. **72**, 3064 (1994).
[6] J. A. Venables, G. D. T. Spiller, and M. Hanbücken, Rep. Prog. Phys. **47**, 399 (1984).
[7] S. Stoyanov and D. Kaschiev, in *Current Topics in Materials Science*, edited by E. Kaldis (North-Holland, Amsterdam, 1981), Vol. 7, p. 69.
[8] J. Villain, A. Pimpinelli, L.-H. Tang, and D. Wolf, J. Phys. (France) I **2**, 2107 (1992).
[9] M. C. Bartelt and J. W. Evans, Phys. Rev. B **46**, 12 675 (1992).
[10] M. C. Bartelt, M. C. Tringides, and J. W. Evans, Phys. Rev. B **47**, 13 891 (1993).
[11] M. C. Bartelt and J. W. Evans, Surf. Sci. **298**, 421 (1993).
[12] T. Nagatani, J. Phys. Soc. Jpn. **62**, 981 (1993).
[13] L.-H. Tang, J. Phys. (France) I **3**, 935 (1993).
[14] G. T. Barkema, O. Biham, M. Brennan, D. O. Boerma, and G. Vidali, Surf. Sci. Lett. **306**, L569 (1994).
[15] C. Ratsch, A. Zangwill, P. Šmilauer, and D. D. Vvedensky, Phys. Rev. Lett. **72**, 3194 (1994).
[16] J. G. Amar, F. Family, and P.-M. Lam, Phys. Rev. B **50**, 8781 (1994).
[17] J. G. Amar and F. Family, Phys. Rev. Lett. **74**, 2066 (1995).
[18] G. S. Bales and D. C. Chrzan, Phys. Rev. B **50**, 6057 (1994).
[19] J. A. Blackman and A. Wilding, Europhys. Lett. **16**, 115 (1991).
[20] J. A. Blackman and A. Marshall, J. Phys. A **27**, 725 (1994).
[21] N. V. Brilliantov and P. L. Krapivsky, J. Phys. A **24**, 4787 (1991).

[22] A. A. Lushnikov and M. Kulmala, Phys. Rev. E **52**, 1658 (1995).
[23] J. A. Venables, Philos. Mag. **27**, 697 (1973).
[24] J. W. Evans and M. C. Bartelt, J. Vac. Sci. Technol. A **12**, 1800 (1994).
[25] F. Family and P. Meakin, Phys. Rev. A **40**, 3836 (1989).
[26] J. A. Blackman, Physica A **220**, 85 (1995).
[27] P. A. Mulheran and J. A. Blackman, Philos. Mag. Lett. **72**, 55 (1995).
[28] P. A. Mulheran and J. A. Blackman, Phys. Rev. B **53**, 10 261 (1996).
[29] J. A. Venables and D. J. Ball, Proc. R. Soc. London, Ser. A **332**, 331 (1971).
[30] D. L. Weaire and N. Rivier, Contemp. Phys. **23**, 59 (1984).
[31] D. L. Weaire, J. P. Kermode, and J. Wejchert, Philos. Mag. B **53**, L101 (1986).
[32] P. A. Mulheran, Philos. Mag. Lett. **66**, 219 (1992).